



Suzuki, H., Harrison, C. J., Shimamura, M., Kohchi, T., & Nishihama, R. (2020). Positional cues regulate dorsal organ formation in the liverwort *Marchantia polymorpha*. *Journal of Plant Research*, 2020. <https://doi.org/10.1007/s10265-020-01180-5>

Peer reviewed version

Link to published version (if available):  
[10.1007/s10265-020-01180-5](https://doi.org/10.1007/s10265-020-01180-5)

[Link to publication record in Explore Bristol Research](#)  
PDF-document

This is the author accepted manuscript (AAM). The final published version (version of record) is available online via Springer Verlag at <https://doi.org/10.1007/s10265-020-01180-5> . Please refer to any applicable terms of use of the publisher.

## University of Bristol - Explore Bristol Research

### General rights

This document is made available in accordance with publisher policies. Please cite only the published version using the reference above. Full terms of use are available:  
<http://www.bristol.ac.uk/red/research-policy/pure/user-guides/ebr-terms/>

1 Corresponding author: Ryuichi Nishihama

2 Graduate School of Biostudies, Kyoto University, Kyoto 606-8502, Japan

3 Tel: +81-(0)75-753-6390

4 Fax: +81-(0)75-753-6127

5 E-mail: [nishihama@lif.kyoto-u.ac.jp](mailto:nishihama@lif.kyoto-u.ac.jp)

6  
7 Membership holders of the Botanical Society of Japan:

8 Masaki Shimamura, Takayuki Kohchi, and Ryuichi Nishihama

9  
10 Subject Area:

11 (4) Genetics/Developmental Biology

12  
13 Manuscript information:

14 0 table, 7 color figures, 0 black and white figure, 0 supplemental figures, and 0  
15 supplemental movie.

**Positional cues regulate dorsal organ formation in the liverwort *Marchantia polymorpha***

Hidemasa Suzuki<sup>1</sup>, C. Jill Harrison<sup>2</sup>, Masaki Shimamura<sup>3</sup>, Takayuki Kohchi<sup>1</sup> and  
Ryuichi Nishihama<sup>1</sup>

<sup>1</sup> Graduate School of Biostudies, Kyoto University, Kyoto 606-8502, Japan

<sup>2</sup> School of Biological Sciences, University of Bristol, Bristol BS8 1TQ, U.K.

<sup>3</sup> Graduate School of Integrated Sciences for Life, Hiroshima University, Higashi-Hiroshima 739-8528, Japan

## Abstract

Bryophytes and vascular plants represent the broadest evolutionary divergence in the land plant lineage, and comparative analyses of development spanning this divergence therefore offer opportunities to identify truisms of plant development in general. In vascular plants, organs are formed repetitively around meristems at the growing tips in response to positional cues. In contrast, leaf formation in mosses and leafy liverworts occurs from clonal groups of cells derived from a daughter cell of the apical stem cell known as merophytes, and cell lineage is a crucial factor in repetitive organ formation. However, it remains unclear whether merophyte lineages are a general feature of repetitive organ formation in bryophytes as patterns of organogenesis in thalloid liverworts are unclear. To address this question, we developed a clonal analysis method for use in the thalloid liverwort *Marchantia polymorpha*, involving random low-frequency induction of a constitutively expressed nuclear-targeted fluorescent protein by dual heat-shock and dexamethasone treatment. *M. polymorpha* thalli ultimately derive from stem cells in the apical notch, and the lobes predominantly develop from merophytes cleft to the left and right of the apical cell(s). Sector induction in gemmae and subsequent culture occasionally generated fluorescent sectors that bisected thalli along the midrib and were maintained through several bifurcation events, likely reflecting the border between lateral merophytes. Such thallus-bisecting sectors traversed dorsal air pores and gemma cups, suggesting that these organs arise independently of merophyte cell lineages in response to local positional cues.

## Keywords (4-6 keywords in alphabetical order)

Apical cell, Cell lineage, Clonal analysis, *Marchantia polymorpha*, Merophyte, Sectors



## Introduction

Land plant development is characterized by apical growth, in which stem cells residing in the shoot apical meristem produce new tissues and organs, and changes in stem cell and apical function are linked to the origin of three-dimensional land plant forms and their subsequent diversification (reviewed in Harrison 2017; Moody 2020). Whilst bryophyte meristems are thought to have a single apical cell whose geometry and cleavage patterns determine organ position and plants' overall body plan (Harrison et al. 2009; Parihar 1967), lycophyte and fern meristems have one to a few apical cells (Harrison and Langdale 2010; Harrison et al. 2007; Sanders et al. 2011), and seed plants have multicellular meristems (Korn 2001, 2002; Poethig 1987; Poethig and Szymkowiak 1995). Apical cell daughters in non-seed plants are called 'merophytes' and proliferate to form clonally related cell groups (Douin 1925; Gifford 1983; Korn 1993). In mosses and leafy liverworts, the apical cells produce merophytes which divide to generate leaves or tissues such as epidermis and parenchyma (Crandall-Stotler 1980; Harrison et al. 2009; Parihar 1967; Ruhland 1924). Thus, merophytes serve as a repeating unit of shoot formation, and cell lineage is manifest in organ and tissue development. In contrast to other bryophytes, thalloid liverworts have flattened whole plant bodies in place of forming individual leaves (Crandall-Stotler 1981; Shimamura 2016), and patterns of thallus development and organogenesis are unclear.

The liverwort *Marchantia polymorpha* L. grows as a flattened creeping thallus that periodically bifurcates from the apical notch, which houses cuneate apical cell(s) (Fig. 1a, b; Shimamura 2016; Solly et al. 2017). The duration between consecutive notch bifurcation events is termed the "plastochron", and plastochron 1 covers the period between gemma germination and the first bifurcation (Fig. 1a; Solly et al. 2017). On the dorsal side of the thallus, an assimilation organ, the 'air chamber' (Fig. 1c), and a cup-shaped organ generating vegetative propagules, the 'gemma cup' (Fig. 1d), respectively develop repetitively or periodically. Histological and anatomical studies have shown that

air chamber formation begins with aperture formation at a distance from the apical cells, and then an intercellular space, the ‘air pore’ (Fig. 1b), forms between epidermal cells by cell separation (Fig. 1e; Apostolakos et al. 1982; Ishizaki et al. 2013). Though Apostolakos et al. (1982) concluded from observations of intercellular spaces at the corner of most epidermal cells in *M. paleacea* that air chambers have no distinct mother cell but develop from air pore cells surrounding the initial aperture, direct evidence supporting their conclusion is lacking. In contrast to air pores, gemma cup primordia are evident a few cells away from the apical cells in *M. polymorpha* (Fig. 1f; Barnes and Land 1908) suggesting that dorsal merophytes contribute to gemma cup development. Whether dorsal merophytes are the sole contributor, or other merophytes also contribute to gemma cup development is unclear.

This lack of clarity around dorsal organogenesis is inherent in histological and anatomical approaches which capture static snapshots of a series of dynamic developmental processes, and the difficulties in distinguishing merophyte borders in fully developed tissues. In this study, we used clonal analysis to label cell lineages (Poethig 1987), and found that both air chambers and gemma cups are formed across merophyte boundaries, suggesting that positional cues regulate organogenesis in the liverwort *M. polymorpha*.

## **Materials and Methods**

### **Plant materials and growth condition**

Male accessions of *M. polymorpha*, Takaragaike-1 (Tak-1) were used as wild-type plants. *M. polymorpha* was cultured on half strength Gamborg’s B5 medium containing 1% agar under 50-60  $\mu\text{mol photon m}^{-2} \text{s}^{-1}$  continuous white fluorescent light at 22 °C.

### **Plasmid construction and transformation**

Plasmid pMpGWB337tdTN-GUS was generated by LR recombination between

pMpGWB337tdTN (Sugano et al. 2018) and pENTR-gus (Thermo Fisher Scientific, Waltham, MA, USA) using LR Clonase II (Thermo Fisher Scientific) and used for *Agrobacterium*-mediated transformation of Tak-1 thallus (Kubota et al. 2013). *pro*MpSYPI3B:*mTurquoise2*-MpSYPI3B vector was generated as described in Kanazawa et al. (2016). An *mTurquoise2*-coding sequence was amplified with a primer set, *mTurquoise2\_BamHI\_IF\_Fw* (CCCCTTCACCGGATCATGGTGTCTAAGGGTGAGGAAC) and *mTurquoise2\_BamHI\_IF\_Rv* (GCTGCCGCCGGATCCTTTGTAAAGCTCATCCATTCCG), and then inserted into the BamHI-digested *pro*MpSYPI3B:MpSYPI3B entry vector (Kanazawa et al. 2016) using In-Fusion HD Cloning System (TaKaRa, Shiga, Japan). The resultant entry vector was then introduced into pMpGWB101 (Ishizaki et al. 2015) by LR recombination, and then used for *Agrobacterium*-mediated transformation of pMpGWB337tdTN-GUS plant thallus (Kubota et al. 2013).

## SEM imaging

SEM images were taken with 21-day-old Tak-1 thalli using TM3000 (Hitachi High Technologies, Tokyo, Japan).

## Clonal analysis and fluorescence observation

Cre induction on mature gemmae was performed as follows: gemmae on a plate were treated with 3  $\mu$ L of a solution containing 5  $\mu$ M DEX, air dried for 10 to 20 minutes, and subjected to heat shock by incubating the plate in a 37 °C air incubator for various periods. Cre induction on thalli was performed as follows: 8-day-old thalli were vacuum-infiltrated in a solution containing 5  $\mu$ M DEX, transplanted onto agar media, air dried for 10 to 20 minutes, and then heat-shocked in a 37 °C incubator for 35 to 50 minutes.

Sector-formed thalli were embedded in 6% agar block and sectioned into ~200-

µm-thick slices with LinearSlicer Pro 7(DOSAKA EM, Kyoto, Japan). tdTomato, mTurquoise2, and bright field images in mature gemmae, 1-day-old gemmalings, 6-day-old thalli, and sliced samples were captured with fluorescence microscope BZ-X710 (Keyence, Osaka, Japan) and merged after equal adjustment of contrast and brightness for visibility by the BZ-X Analyzer (Keyence). Thalli were observed with fluorescence dissection microscope Leica M205 C (Leica, Wetzlar, Germany). Obtained images were manually merged by using ImageJ (<https://imagej.nih.gov/ij/>) after contrast and brightness were adjusted for visibility. Contribution of tdTomato-positive and -negative regions to a gemma cup was evaluated by counting the number of serrations existing in each region.

#### **Histochemical assay for GUS activity**

Histochemical assay for GUS activity was performed as described previously (Ishizaki et al. 2012).

### **Results**

#### **Exploitation of clonal analysis system**

To determine how dorsal structures develop, we first established a Cre-*loxP* based clonal sector induction system (Fig. 2a). A construct was designed to constitutively express a floxed  $\beta$ -glucuronidase (*GUS*) gene under the *M. polymorpha* *EF1 $\alpha$*  promoter (*proMpEF1 $\alpha$* ), and conditionally express a Cre-recombinase/glucocorticoid receptor (GR) fusion protein under a *M. polymorpha* heat-shock promoter, *MpHSP17.8A1* (Fig. 2a; Nishihama et al. 2016). The rationale for sector induction was that, following heat shock and dexamethasone (DEX) treatment, the Cre protein would excise the *GUS* gene allowing expression of a nuclear targeted red fluorescent protein, tdTomato-NLS, under *proMpEF1 $\alpha$*  (Sugano et al. 2018). Two elements to control conditional expression of the *Cre* gene were included to avoid leaky excision of the floxed region. This system was

expected to mark clonal sectors negatively by the absence of GUS staining or positively by the presence of red fluorescent signal (Fig. 2b).

Clonal analysis requires the production of many sectors induced randomly at different stages of development, and there is therefore an optimal frequency of sector induction. Whereas a low frequency of induction generates too few sectors to generate sufficient data for analysis, a high frequency of induction can induce overlapping sectors, becoming uninformative. To optimise the frequency of sector induction and analyse organogenesis in gemmalings and thalli, we first treated gemmae with a solvent control solution or a solution containing 5  $\mu$ M DEX, and then heat-shocked gemmae for different periods of time at 37 °C. We subsequently examined gemmae by fluorescence microscopy. The frequency of cells showing fluorescence in the gemma increased as the duration of the heat-shock increased in DEX-treated gemmae, but increased to a lesser extent in untreated gemmae such that sectors were absent in gemmae with no heat shock and present in almost all cells in gemmae that were heat-shocked for 80 minutes (Fig. 2c). A 30-40 minute heat-shock induced sectors at a moderate frequency that was compatible with the requirements of clonal analysis, and was thus used in further experiments, unless otherwise noted.

### **Lateral merophytes bisect thallus lobes**

Cre induction in mature gemmae and subsequent plant development caused sector formation in various patterns. Some sectors bisected the thallus lobe (Fig. 3), spanning the dorsal to ventral axis (Fig. 3a), and such sectors persisted through several bifurcation events with well-defined sharp borders (Fig. 3b), consistent with a lateral merophyte origin (see merophyte sectors in Harrison et al. 2007; Harrison et al. 2009; Sanders et al. 2011 for comparison).

### **Air pores are formed independently of merophyte cell lineage**

Observations of air chambers at sector junctions showed an overlap with the edge of some air chambers, but other air chambers were divided into fluorescence-positive and -negative regions (Fig. 4a). Whilst the former constituted approximately half of cases, amongst the latter, a pattern where the sector border was positioned in the centre of the air pore predominated, but in some cases sectors were off centre (Fig. 4b). Only small proportion of air chambers had sectors that did not cross the air pore (Fig. 4b). Observation in an early developmental stage revealed sectors that covered not only entire air chambers but also half air chambers with the sector border positioned in the centre of the air pore (Fig. 4c). These data suggest that air chambers can be formed either within a merophyte cell lineage or between merophyte cell lineages (see Fig. 7).

### **Gemma cups are a multi-lineage-comprised organ**

Next, we observed gemma cups that had formed during the second to fourth plastochrons (Fig. 5a; Solly et al. 2017) on thalli with persistent bisecting sectors (Fig. 3b) and found that such gemma cups were also bisected by the sectors and sometimes contained both fluorescence-positive and -negative gemmae (Fig. 5b). Not only the wall, but also the floor of gemma cups (where gemma initials arise) were separated by such sectors (Fig. 5c). These results suggest that gemma cups are not derived from a single merophyte, but multiple merophytes. Contribution of a fluorescence-positive region (or conversely a fluorescence-negative region) to a gemma cup varied depending on the timing of its formation relative to notch bifurcation; those formed during the second and fourth plastochrons showed a range of contributions from 0 to 100%, while those formed during the third plastochron showed approximately 50% contribution (Fig. 5d). These results suggest that gemma cups initiate from two or more cells at the boundary between thallus lobes arising from lateral merophytes, that the process of bifurcation has some inherent variability, and that positional cues are important in gemma cup development.

Gemma cup initials are first recognizable a few cells away from the apical cells (Barnes and Land 1908), and the dorsal merophyte is believed to participate in gemma cup development. However, this idea has never been demonstrated experimentally. Because gemma cups are never formed during the first plastochron (Fig. 5a), we induced Cre-*loxP* recombination on 8-day-old thalli, during the second plastochron. Sectors that were several cells wide emerged along the midrib during the third plastochron. These line-shaped sectors were later separated from the apical notches (Fig. 6a), and were only present on the dorsal surface (Fig. 6b), suggesting a dorsal merophyte origin. Such sectors also overlapped with gemma cups (Fig. 6c), suggesting a minor contribution of dorsal merophytes to gemma cup development. Taken together, these observations suggest that gemma cups arise from dorsal merophytes and dorsal derivatives of lateral merophytes (Fig. 7).

## Discussion

Clonal analysis has considerably contributed to understanding plant development. Methodologies for clonal analysis widely vary, involving ploidy changes induced by colchicine (Satina et al. 1940), activation of *GUS* transgene expression by random or heat-shock-mediated removal of transposons (Dolan et al. 1994; Kidner et al. 2000; Scheres et al. 1994), inactivation of *GUS* transgene expression by heat-shock-mediated Cre-*loxP* excision (Saulsberry et al. 2002), pale green pigmentation or chloroplast biogenesis defects induced by X-ray irradiation (Harrison et al. 2007; Harrison et al. 2009), utilisation of variegated species (Sanders et al. 2011), and so on. This paper reports a new clonal analysis method for *M. polymorpha*, which we anticipate will contribute to understanding patterns of *M. polymorpha* development. For the purpose of lineage visualisation, our method could be further improved by incorporating a multi-colour system such as Brainbow (Livet et al. 2007) and Brother of Brainbow (Wachsman et al. 2011). Clonal analysis could be utilised to analyse gene functions in the context of

specific cell lineages or positions (Heidstra et al. 2004; Sieburth et al. 1998). By taking advantage of live imaging, our method could be widely applied to conditional genetic analyses using various molecular tools established in *M. polymorpha* (Ishizaki et al. 2015; Kopischke et al. 2017; Mano et al. 2018; Nishihama et al. 2016; Sugano et al. 2018).

Here, Cre induction in mature gemmae and subsequent growth occasionally generated sectors that bisected thalli and were maintained through bifurcation events, and such sectors are likely to arise by Cre induction in lateral merophytes or apical cells. Some air pores on such sectors were divided into fluorescence-positive and -negative regions (Fig. 4). Air chambers are known to arise from initial apertures that are formed in the limited area around an apical cell, and aperture-surrounding cells later develop into air pores (Apostolakos et al. 1982). Our analysis demonstrated that air pores could emerge across merophyte boundaries as well as within single merophytes, suggesting that air pore formation does not depend on cell lineages but on local cues around the notch (Fig. 7). We further found that most air-chamber sectors traversed air pores, suggesting that cells that constitute air chambers are derived from initial aperture-surrounding cells, which is consistent with the conclusions by Apostolakos et al. (1982).

Gemma cups were also divided by thallus-bisecting sectors (Fig. 5), suggesting that no single initial cell gives rise to gemma cups and that gemma cup development is controlled by local cues. Our observations that the boundary of thallus-bisecting sectors represents the border of lateral merophytes and that dorsal merophyte sectors are incorporated into gemma cups (Fig. 6) demonstrate that gemma cups derive from both dorsal and lateral merophytes (Fig. 7). Though the mechanisms that allow lateral merophytes to contribute differentially to gemma cup formation (Fig. 5d) are unclear, the degree of lateral proliferation of lateral and dorsal merophyte cells may vary depending on the plastochron, or due to plasticity. Recently, an R2R3-type MYB transcription factor, GEMMA CUP-ASSOCIATED MYB1 (GCAM1), was reported to play an essential role in gemma cup formation (Yasui et al. 2019). *GCAM1* is expressed in the notch and the



gemma cup floor and is proposed to maintain dorsal cells near the apical cell in undifferentiated status for gemma cup formation (Yasui et al. 2019). Clarification of the early expression pattern of *GCAMI* in relation to dorsal and lateral merophytes could provide clues to the mechanism of gemma cup formation.

In angiosperms, tissue and organ differentiation is based on cell fates that are determined by positional signals (Kidner et al. 2000; Reinhardt et al. 2005; Scheres 2001; Scheres et al. 1994; Sussex 1951, 1954; van den Berg et al. 1995). Flow of the phytohormone auxin specifies the site of cell differentiation for organ formation, such as leaves and lateral roots. Cell lineages also contribute to the formation of tissue layers, such as the tunica and corpus layers of the shoot apical meristem and the radial layers of root tissues, but their identities are often specified by cell-cell communications with other lineage cells. In *M. polymorpha*, auxin signaling via transcriptional regulation plays critical roles in the development of gemmae through regulation of cell division patterns (Kato et al. 2017). The intermerophyte pattern of organogenesis revealed in this study suggests that similar local signal-mediated cell-fate determination operates in *M. polymorpha*. In contrast, lateral organs in leafy bryophytes arise from merophyte cell lineages with clear histological boundaries (Crandall-Stotler 1980; Harrison et al. 2009; Parihar 1967; Ruhland 1924). Changes in the cell fate determination system may have led to the morphological diversification of complex thalloid liverworts.

## Acknowledgements

We thank Takashi Ueda and Takehiko Kanazawa for kindly providing the Mp*SYP13B* entry vector. We thank Shohei Yamaoka, Sakiko Ishida, Akari Ito, Moe Kagao, Masaya Tsumura, Runa Sato and Yuki Sato for helpful discussion. This work was supported by the Japan Society for the Promotion of Science KAKENHI (grant number JP18J12698 to H.S.), the Ministry of Education, Culture, Sports, Science & Technology KAKENHI (grant number 18H04836 to R.N.), and SPIRITS 2017 of Kyoto University to R.N.

## References

- Apostolakos P, Galatis B, Mitrakos K (1982) Studies on the development of the air pores and air chambers of *Marchantia paleacea*. 1. Light microscopy. *Ann Bot* 49:377-396
- Barnes CR, Land WJG (1907) Bryological papers. I. The origin of air chambers. *Bot Gaz* 44:197-213
- Barnes CR, Land WJG (1908) Bryological papers. II. The origin of the cupule of *Marchantia*. *Bot Gaz* 46:401-409
- Crandall-Stotler B (1980) Morphogenetic designs and a theory of bryophyte origins and divergence. *BioScience* 30:580-585
- Crandall-Stotler B (1981) Morphology/anatomy of hepatics and anthocerototes. J. Cramer, Vaduz, Lichtenstein
- Dolan L, Duckett CM, Grierson C, Linstead P, Schneider K, Lawson E, Dean C, Poethig S, Roberts K (1994) Clonal relationships and cell patterning in the root epidermis of *Arabidopsis*. *Development* 120:2465-2474
- Douin C (1925) La théorie des initiales chez les Hépatiques à feuilles. *Bull Soc Bot Fr* 72:565-591
- Gifford EMJ (1983) Concept of apical cells in bryophytes and pteridophytes. *Ann Rev Plant Physiol* 34:419-440
- Harrison CJ (2017) Development and genetics in the evolution of land plant body plans. *Phil Trans R Soc B* 372:20150490
- Harrison CJ, Langdale JA (2010) Comment: The developmental pattern of shoot apices in *Selaginella kraussiana* (Kunze) A. Braun. *Int J Plant Sci* 171:690-692
- Harrison CJ, Rezvani M, Langdale JA (2007) Growth from two transient apical initials in the meristem of *Selaginella kraussiana*. *Development* 134:881-889
- Harrison CJ, Roeder AH, Meyerowitz EM, Langdale JA (2009) Local cues and asymmetric cell divisions underpin body plan transitions in the moss *Physcomitrella patens*. *Curr Biol* 19:461-471
- Heidstra R, Welch D, Scheres B (2004) Mosaic analyses using marked activation and

324 deletion clones dissect *Arabidopsis* SCARECROW action in asymmetric cell division.  
325 Genes Develop 18:1964-1969

326 Ishizaki K, Mizutani M, Shimamura M, Masuda A, Nishihama R, Kohchi T (2013)  
327 Essential role of the E3 ubiquitin ligase NOPPERABO1 in schizogenous intercellular  
328 space formation in the liverwort *Marchantia polymorpha*. Plant Cell 25:4075-4084

329 Ishizaki K, Nishihama R, Ueda M, Inoue K, Ishida S, Nishimura Y, Shikanai T, Kohchi T  
330 (2015) Development of Gateway binary vector series with four different selection  
331 markers for the liverwort *Marchantia polymorpha*. PLOS ONE 10:e0138876

332 Ishizaki K, Nonomura M, Kato H, Yamato KT, Kohchi T (2012) Visualization of auxin-  
333 mediated transcriptional activation using a common auxin-responsive reporter system in  
334 the liverwort *Marchantia polymorpha*. J Plant Res 125:643-651

335 Kanazawa T, Era A, Minamino N, Shikano Y, Fujimoto M, Uemura T, Nishihama R,  
336 Yamato KT, Ishizaki K, Nishiyama T, Kohchi T, Nakano A, Ueda T (2016) SNARE  
337 molecules in *Marchantia polymorpha*: unique and conserved features of the membrane  
338 fusion machinery. Plant Cell Physiol 57:307-324

339 Kato H, Kouno M, Takeda M, Suzuki H, Ishizaki K, Nishihama R, Kohchi T (2017) The  
340 roles of the sole activator-type auxin response factor in pattern formation of *Marchantia*  
341 *polymorpha*. Plant Cell Physiol 58:1642-1651

342 Kidner C, Sundaresan V, Roberts K, Dolan L (2000) Clonal analysis of the *Arabidopsis*  
343 root confirms that position, not lineage, determines cell fate. Planta 211:191-199

344 Kopischke S, Schussler E, Althoff F, Zachgo S (2017) TALEN-mediated genome-editing  
345 approaches in the liverwort *Marchantia polymorpha* yield high efficiencies for targeted  
346 mutagenesis. Plant Methods 13:20

347 Korn RW (1993) Apical cells as meristems. Acta Biotheor 41:175-189

348 Korn RW (2001) Analysis of shoot apical organization in six species of the Cupressaceae  
349 based on chimeric behavior. Am J Bot 88:1945-1952

350 Korn RW (2002) Chimeric patterns in *Juniperus chinensis* ‘Torulosa Variegata’  
351 (Cupressaceae) expressed during leaf and stem formation. Am J Bot 89:758-765

352 Kubota A, Ishizaki K, Hosaka M, Kohchi T (2013) Efficient *Agrobacterium*-mediated

353 transformation of the liverwort *Marchantia polymorpha* using regenerating thalli. Biosci  
354 Biotechnol Biochem 77:167-172

355 Livet J, Weissman TA, Kang H, Draft RW, Lu J, Bennis RA, Sanes JR, Lichtman JW  
356 (2007) Transgenic strategies for combinatorial expression of fluorescent proteins in the  
357 nervous system. Nature 450:56-62

358 Mano S, Nishihama R, Ishida S, Hikino K, Kondo M, Nishimura M, Yamato KT, Kohchi  
359 T, Nakagawa T (2018) Novel gateway binary vectors for rapid tripartite DNA assembly  
360 and promoter analysis with various reporters and tags in the liverwort *Marchantia*  
361 *polymorpha*. PLOS ONE 13:e0204964

362 Moody L (2020) Three-dimensional growth: A developmental innovation that facilitated  
363 plant terrestrialization. J Plant Res. <https://doi.org/10.1007/s10265-020-01173-4>

364 Nishihama R, Ishida S, Urawa H, Kamei Y, Kohchi T (2016) Conditional gene  
365 expression/deletion systems for *Marchantia polymorpha* using its own heat-shock  
366 promoter and Cre/loxP-mediated site-specific recombination. Plant Cell Physiol 57:271-  
367 280

368 Parihar NS (1967) An introduction to Embryophyta volume I: Bryophyta. Indian  
369 Universities Press, Allahbad

370 Poethig RS (1987) Clonal analysis of cell lineage patterns in plant development. Am J  
371 Bot 74:581-594

372 Poethig RS, Szymkowiak EJ (1995) Clonal analysis of leaf development in maize.  
373 Maydica (Italy) 40:67-76

374 Reinhardt D, Frenz M, Mandel T, Kuhlemeier C (2005) Microsurgical and laser ablation  
375 analysis of leaf positioning and dorsoventral patterning in tomato. Development 132:15-  
376 26

377 Ruhland W (1924) Musci. Allgemeiner Teil. Verlag von Wilhelm Engelmann, Leipzig

378 Sanders HL, Darrah PR, Langdale JA (2011) Sector analysis and predictive modelling  
379 reveal iterative shoot-like development in fern fronds. Development 138:2925-2934

380 Satina S, Blakeslee AF, Avery AG (1940) Demonstration of the three germ layers in the  
381 shoot apex of datura by means of induced polyploidy in periclinal chimeras. Am J Bot

382 27:895-905

383 Saulsberry A, Martin PR, O'Brien T, Sieburth LE, Pickett FB (2002) The induced sector  
384 *Arabidopsis* apical embryonic fate map. *Development* 129:3403-3410

385 Scheres B (2001) Plant Cell Identity. The role of position and lineage. *Plant Physiol*  
386 125:112-114

387 Scheres B, Wolkenfelt H, Willemsen V, Terlouw M, Lawson E, Dean C, Weisbeek P  
388 (1994) Embryonic origin of the *Arabidopsis* primary root and root meristem initials.  
389 *Development* 120:2475-2487

390 Shimamura M (2016) *Marchantia polymorpha*: taxonomy, phylogeny and morphology of  
391 a model system. *Plant Cell Physiol* 57:230-256

392 Sieburth LE, Drews GN, Meyerowitz EM (1998) Non-autonomy of *AGAMOUS* function  
393 in flower development: use of a *Cre/loxP* method for mosaic analysis in *Arabidopsis*.  
394 *Development* 125:4303

395 Solly JE, Cuniffe NJ, Harrison CJ (2017) Regional growth rate differences specified by  
396 apical notch activities regulate liverwort thallus shape. *Curr Biol* 27:16-26

397 Sugano SS, Nishihama R, Shirakawa M, Takagi J, Matsuda Y, Ishida S, Shimada T, Hara-  
398 Nishimura I, Osakabe K, Kohchi T (2018) Efficient CRISPR/Cas9-based genome editing  
399 and its application to conditional genetic analysis in *Marchantia polymorpha*. *PLOS ONE*  
400 13:e0205117

401 Sussex IM (1951) Experiments on the cause of dorsiventrality in leaves. *Nature* 167:651-  
402 652

403 Sussex IM (1954) Experiments on the cause of dorsiventrality in leaves. *Nature* 174:351-  
404 352

405 van den Berg C, Willemsen V, Hage W, Weisbeek P, Scheres B (1995) Cell fate in the  
406 *Arabidopsis* root meristem determined by directional signalling. *Nature* 378:62-65

407 Wachsman G, Heidstra R, Scheres B (2011) Distinct cell-autonomous functions of  
408 *RETINOBLASTOMA-RELATED* in *Arabidopsis* stem cells revealed by the Brother of  
409 Brainbow clonal analysis system. *Plant Cell* 23:2581-2591

410 Yasui Y, Tsukamoto S, Sugaya T, Nishihama R, Wang Q, Kato H, Yamato KT, Fukaki H,  
411 Mimura T, Kubo H, Theres K, Kohchi T, Ishizaki K (2019) GEMMA CUP-  
412 ASSOCIATED MYB1, an ortholog of axillary meristem regulators, is essential in  
413 vegetative reproduction in *Marchantia polymorpha*. Curr Biol 29:3987-3995  
414

## Figures and Figure legends

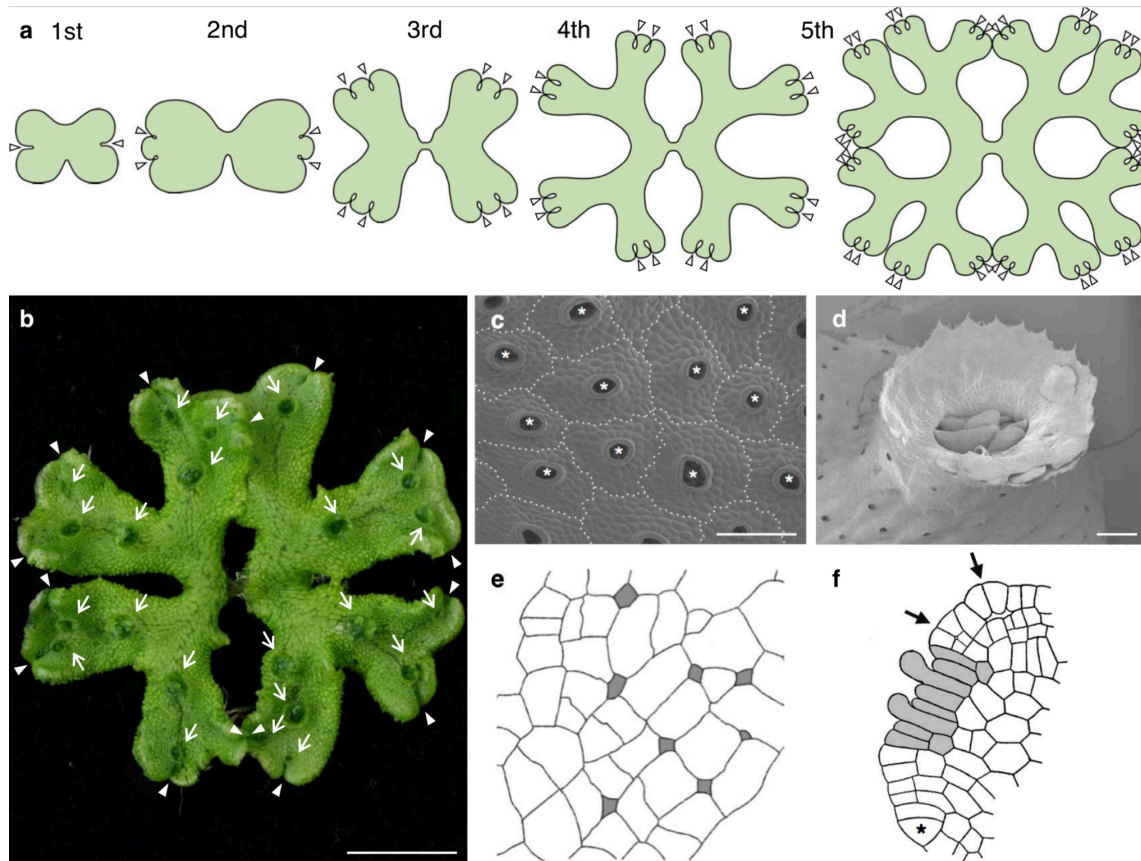


**Fig. 1** Notch bifurcations and dorsal structures of the thallus of *M. polymorpha*.

**a** Scheme of bifurcating thalli in the  $n$ th plastochron stages with exponentially increasing apical notches. Arrowheads indicate apical notches. **b** A 21-day-old *M. polymorpha* thallus in the 4th plastochron. Arrows and Arrowheads indicate gemma cups and apical notches, respectively. Scale bar = 5 mm. **c** Scanning electron microscope (SEM) image of air chambers with one air pore each. Dotted lines and asterisks indicate border of air chambers and air pores, respectively. Scale bar = 200  $\mu$ m. **d** SEM image of a gemma cup with serrated edges. Scale bar = 500  $\mu$ m. **e** Surface view of initial apertures (grey) which develop into an air pore (Redrawn from Apostolakos et al. (1982)). **f** Vertical longitudinal view of the apical cell and its derivatives. An asterisk, grey area, arrows indicate an apical

cell, gemma cup initial region, young air chambers, respectively (Redrawn from Barnes and Land (1908)). It should be noted that Barnes and Land proposed that initiation of air chambers occurs internally at the intersection of daughter cells from a single mother cell (Barnes and Land 1907), and that the present picture is drawn as such.

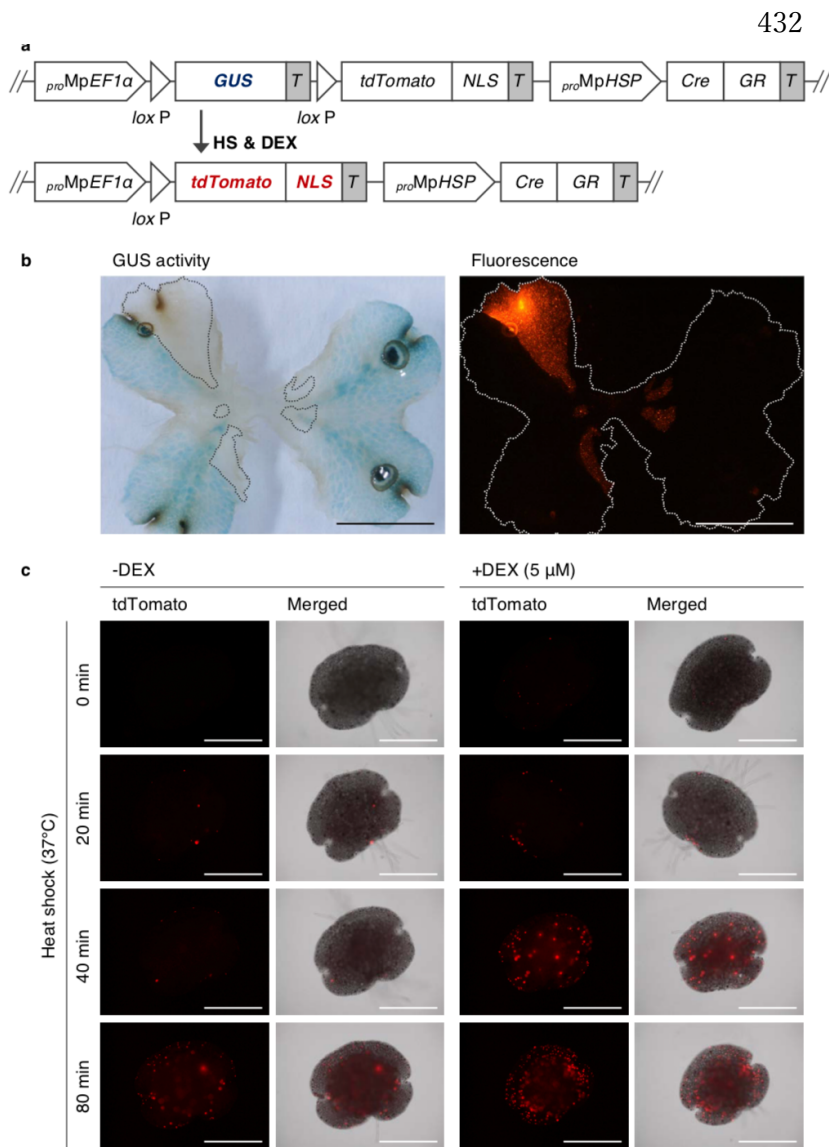


**Fig. 2** Clonal analysis system in *M. polymorpha*.

**a** Schematic diagram of the construct used in clonal analysis. In the standard state (top), *tdTomato-NLS* is not transcribed due to an upstream terminator. Heat shock (HS) and dexamethasone (DEX) treatments induce Cre-*loxP*-mediated excision of the *loxP*-



flanked region (bottom), which in turn constitutively switches on *tdTomato-NLS*. *T*:  
*NOS* terminator. **b** Reciprocal formation of GUS and tdTomato sectors. This plant was  
treated with HS and DEX in mature gemmae and grown for 14 days. Grey dotted lines  
on the left panel indicates approximate position of tdTomato-positive sectors. A white  
dotted line on the right panel indicate an outline of the thallus. Bars = 5 mm. **c**  
Efficiency of Cre-*loxP* recombination. Mature gemmae of the transgenic line were  
treated with or without DEX, and then heat-shocked for 0, 20, 40, or 80 min in a 37 °C  
incubator. One day after the induction, the plants showed fluorescence in a HS- and  
DEX-dependent manner. Scale bars = 500 µm.

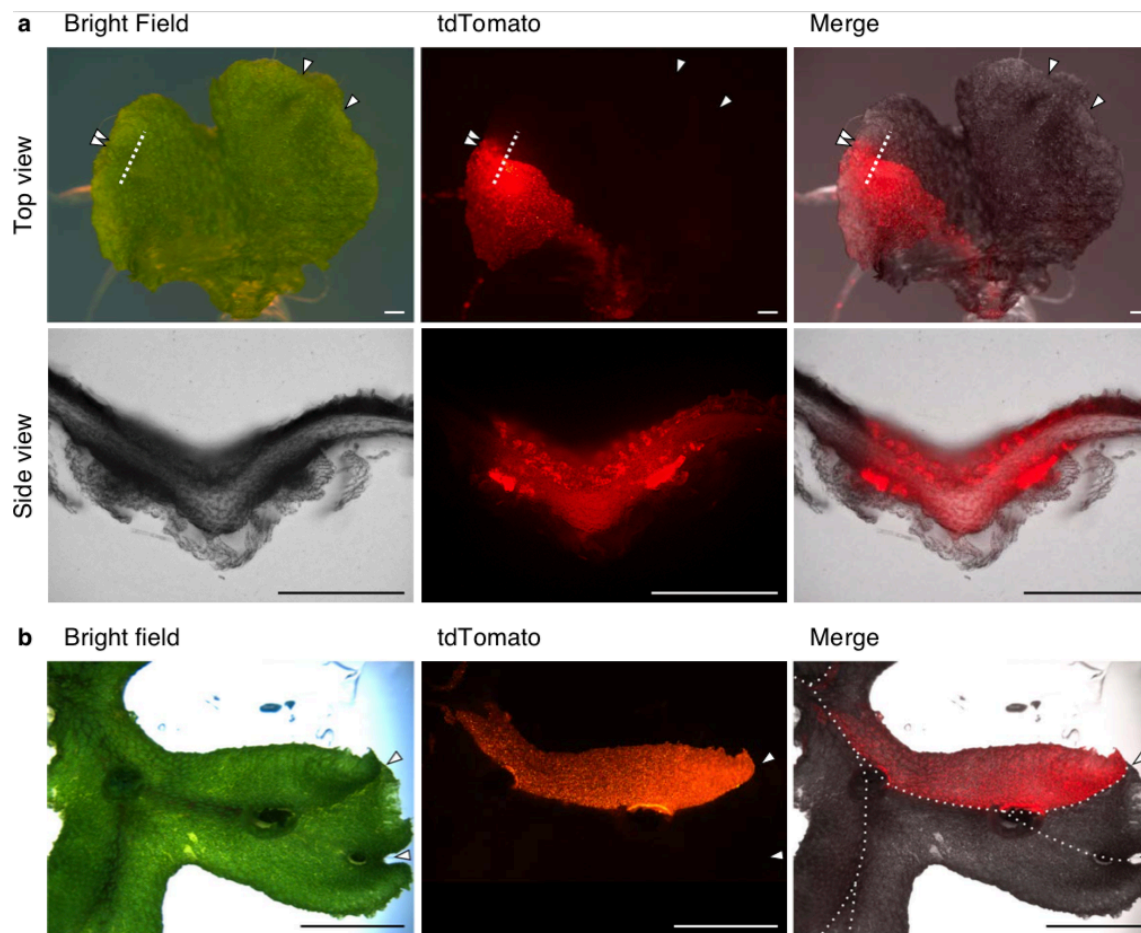


**Fig. 3** Sectors that bisect thallus lobes

**a** Top (upper row) and side (lower row) view of a sector bisecting a thallus lobe in the third plastochron of a 13-day-old plant. Dotted lines indicate the approximate position of the side-view section (basal side observed). Arrowheads indicate apical notches. Scale bars = 500  $\mu$ m. **b** A sector bisecting a thallus lobe from the base to an apical notch in the fourth plastochron of a 23-day-old plant. Dotted lines indicate midribs. Arrows and arrowheads indicate gemma cups and apical notches, respectively. Scale bar = 5 mm.

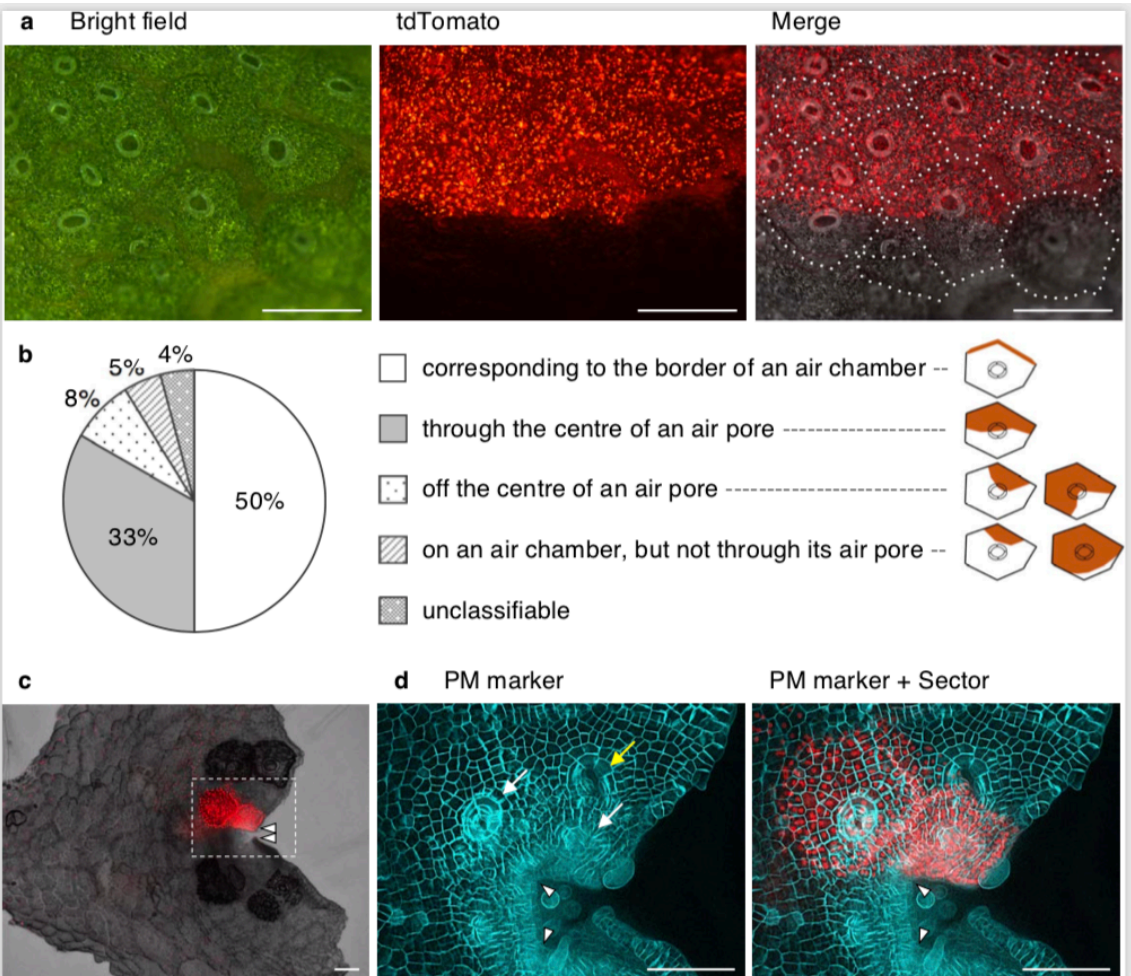


**Fig. 4** Division of air pores and air chambers by thallus-bisecting sectors

**a** A tdTomato-positive sector on dorsal surface of a thallus. Dotted lines in the merged picture indicate the edges of air chambers. Scale bars = 500  $\mu$ m. **b** Ratio of relative position of sectors to an air pores (see graph legends and schematic illustrations).  $n = 192$

air pores from 10 merophyte sectors. **c, d** A notch-adjacent sector in the second plastochron of a 6-day-old plant (**c**) and its magnified view around the notch within the white dotted rectangle (**d**). As a plasma membrane (PM) marker, mTurquoise2-tagged MpSYP13B (Kanazawa et al. 2016) was co-expressed under the regulation of its native promoter. Arrowheads indicate apical notches. White and yellow arrows indicate air pores formed within and across a sectorized region, respectively. Scale bars = 100  $\mu$ m.

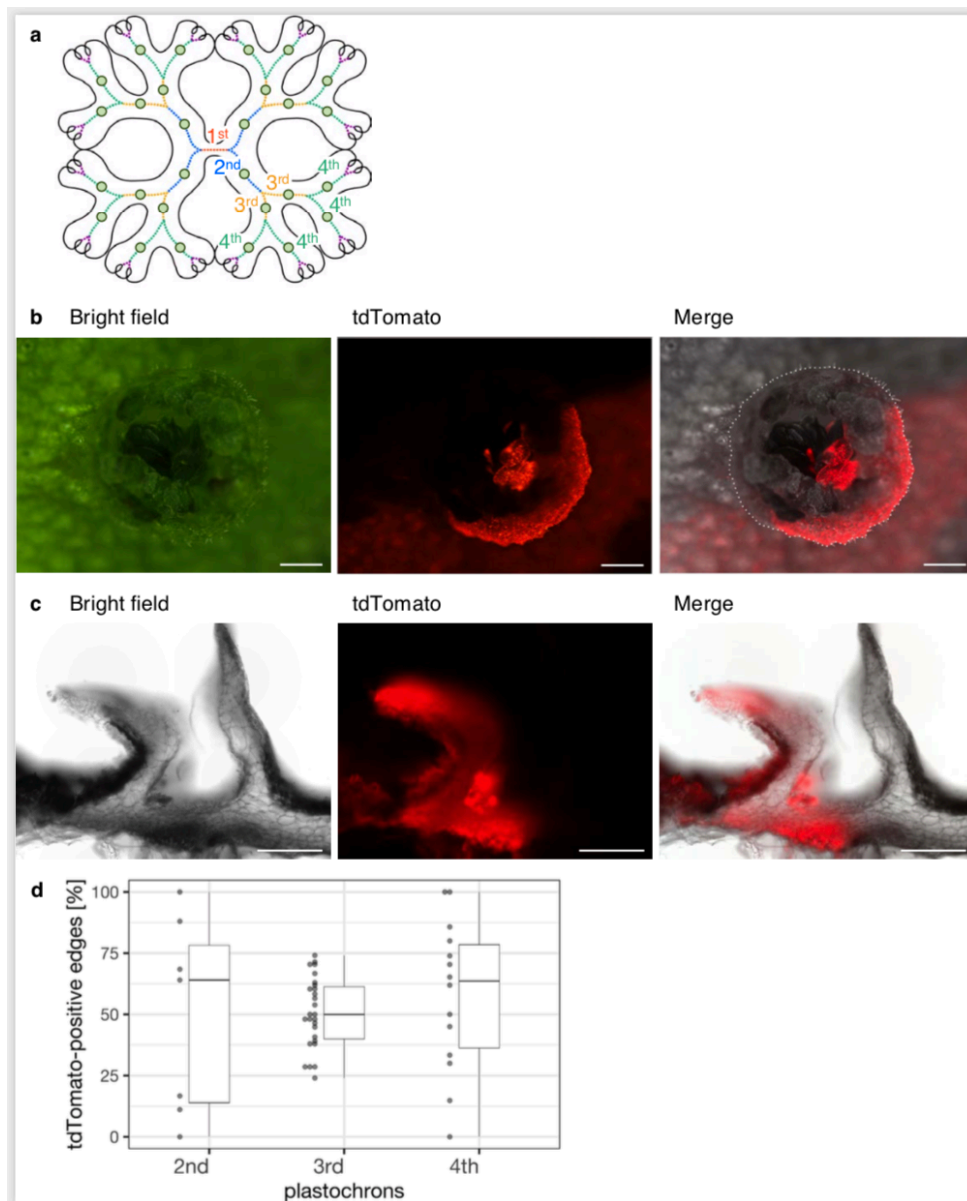


**Fig. 5** Division of gemma cups by thallus-bisecting sectors

**a** Correlation between gemma cup positions and plastochron numbers. Circles and differently coloured lines indicate gemma cups and the growth phase of each plastochron, respectively. Gemma cups were never formed during the 1st plastochron under the growth conditions we used. **b** A gemma cup bisected by a merophyte sector. A white dotted line in the merged picture indicates an outline of the gemma cup. Scale bars = 500  $\mu$ m. **c** Vertical transverse section of a gemma cup on a merophyte sector. Scale bars = 500  $\mu$ m. **d** Dot- and box-plots for the ratio of tdTomato-positive serration edges in a gemma cup formed on a thallus-bisecting sector. The dots are individual values. The bottom and top of each box represent the first and third quartiles, respectively. The band inside the box is the median.

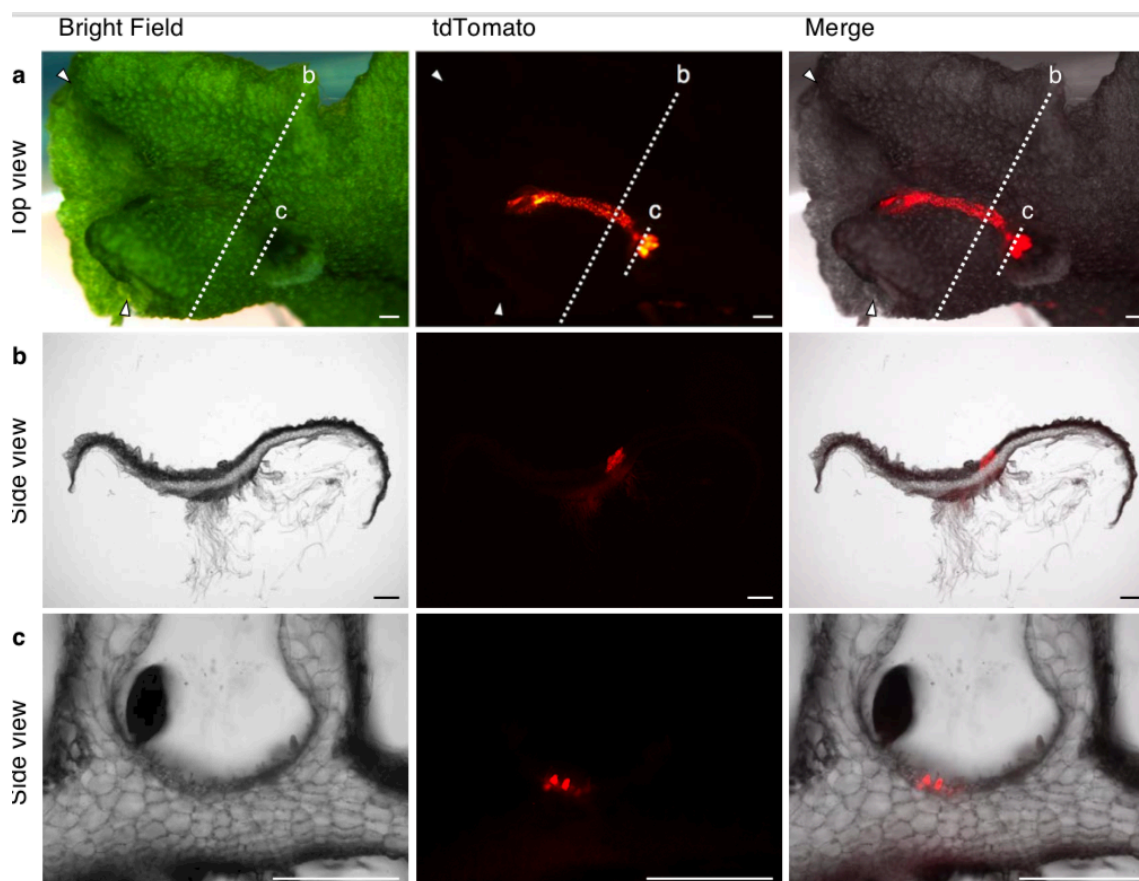


**Fig. 6** Division of gemma cups by dorsal merophyte sectors



**a–c** Top (**a**) and side (**b** and **c**) views of a dorsal line-shaped sector along the midrib that includes a part of gemma cup in the third plastochron of a 23-day-old plant. Scale bars = 500  $\mu\text{m}$ . White dotted lines in **a** indicate the approximate positions of the side-view sections in **b** and **c** (basal sides observed). Arrowheads in **a** indicate apical notches.

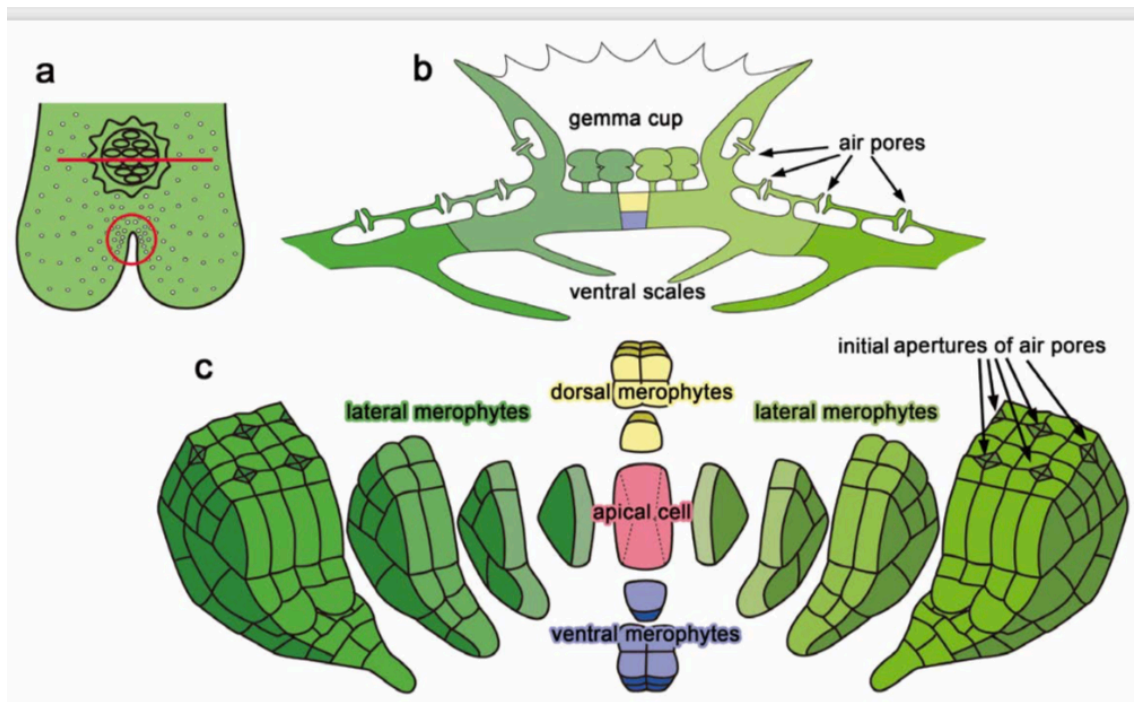


**Fig. 7** Models of dorsal organ formation in relation to merophytes  
Red line and circle in **a** indicate the positions of schematic illustrations for a gemma cup part (vertical transverse section, **b**) and the notch (front view, **c**). Cells in red, yellow, purple, and different levels of green colors in **b** and **c** indicate an apical cell, dorsal merophytes, ventral merophytes, and lateral merophytes, respectively.